

Synthesis of Pt Nanoparticles in Water-in-Oil Microemulsion: Effect of HCl on Their Surface Structure

Roberto A. Martínez-Rodríguez,[†] Francisco J. Vidal-Iglesias,[‡] José Solla-Gullón,^{*‡} Carlos R. Cabrera,[†] and Juan M. Feliu[‡]

[†]NASA-URC Center for Advanced Nanoscale Materials (CANM), Department of Chemistry, University of Puerto Rico, Río Piedras Campus, P.O. Box 23346, San Juan 00931-3346, Puerto Rico

[‡]Institute of Electrochemistry, University of Alicante, Ap. 99, 03080 Alicante, Spain

S Supporting Information

ABSTRACT: The synthesis of shape-controlled nanoparticles is currently a hot research topic. However, from an applied point of view, there is still a lack of easy, cheap, and scalable methodologies. In this communication we report, for the first time, the synthesis of cubic platinum nanoparticles with a very high yield using a water-in-oil microemulsion method, which unlike others, such as the colloidal method, fulfills the previous requirements. This shape/surface structure control is determined by the concentration of HCl in the water phase of the microemulsion. The results reported here show that the optimal HCl percentage in the water phase is about 25% to obtain the highest amount of cubic nanostructures. Ammonia electro-oxidation is used as a surface structure sensitive reaction to illustrate HCl surface structure effects. Moreover, in situ electrochemical characterization has been performed to study the nanoparticle surface structure.

The electrochemical properties of nanoparticles are mainly determined by their bulk/surface composition, size, geometry, and surface structure.^{1–9} This last parameter is of great importance, as many electrochemical reactions of interest are well-established to be structure sensitive. That is why during the past decade there has been an increasing interest over the control of metal nanoparticle shape,² with the idea that through its control the arrangement of the atoms at the surface can be tuned and consequently its catalytic activity can be modified. From the pioneering work of El-Sayed et al.,⁷ in which cubic and tetrahedral Pt nanoparticles were prepared with H₂ in the presence of sodium polyacrylate, many other methods have been developed. Thus, shape-controlled nanoparticles of different metals as well as core–shell and alloyed structures have been successfully synthesized. However, due to its unique catalytic properties, Pt has been the metal attracting the widest attention by far.^{3–7} Unfortunately, these synthetic procedures always require the presence of capping agents and most of them also need high temperatures or long growth times, which make them difficult to scale up. Consequently, the development of a fast, easy, cost-effective, room-temperature, and scalable procedure of synthesis of shape-controlled metal nanoparticles would be of great importance.

Water-in-oil microemulsion is, among others, a very interesting candidate because it allows the synthesis of a wide number of nanoparticles of uniform size at room temperature in a very fast and economical way. Unfortunately, the control over the shape/surface structure of the nanoparticles, in particular noble-metal nanoparticles (Pt, Au, Pd, etc.), is still very limited. In this sense, in previous contributions, we have shown that by using different surface modifiers (iodine and bromide) for Au nanoparticles^{10,11} or by changing the strength of the reducing agent (hydrazine or NaBH₄) for Pt nanoparticles,¹¹ both prepared in water-in-oil microemulsion, we were able to induce slight modifications in the surface structure of the nanoparticles, although without significant changes in their quasi-spherical shape as observed by TEM.

In this contribution, we show for the first time that cubic Pt nanoparticles can be easily prepared using a water-in-oil microemulsion by including specific amounts of HCl in the water phase of the microemulsion. In addition, the percentage of HCl will control the final shape of the nanoparticles. The size and shape of such Pt nanoparticles were evaluated by TEM measurements, and the surface structure was characterized by using different electrochemical probes. Finally, the electrocatalytic properties of the nanoparticles were tested using ammonia electro-oxidation in alkaline medium, which has shown to be extremely sensitive to the presence of (100) surface sites.^{12–16}

Pt nanoparticles were synthesized by reducing H₂PtCl₆ with sodium borohydride using a water-in-oil (w/o) microemulsion by a methodology similar to that previously reported.¹⁷ (experimental details are included in the Supporting Information). This procedure allowed us to easily clean the nanoparticles while preserving their initial surface structure. Different amounts of HCl (from 0 to 37%) were incorporated in the water phase of the microemulsion. Irrespective of the amount of HCl, the complete reduction took place in a few minutes, which was indicated by a color change of the solution from light yellow to black. After complete reduction, the nanoparticles were collected and cleaned as described previously and stored in an ultrapure water suspension.¹⁷

Figure 1 shows the voltammetric response of a collection of Pt nanoparticles prepared with different amounts of HCl obtained

Received: November 22, 2013

Published: January 14, 2014

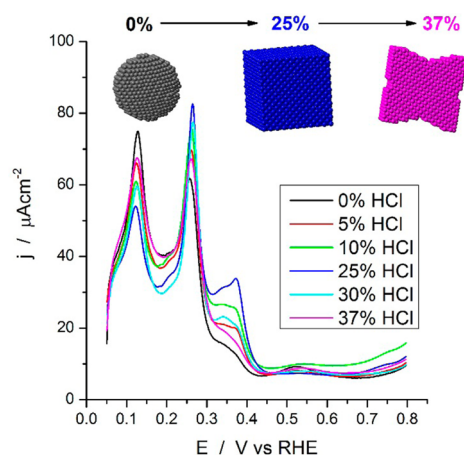


Figure 1. Voltammetric profile for platinum nanoparticles prepared by water-in-oil microemulsion in the presence of different amounts of HCl: test solution, 0.5 M H₂SO₄; scan rate, 50 mV s⁻¹.

in 0.5 M H₂SO₄. It is well-established that the particular voltammetric profile in the so-called hydrogen region is directly related to their specific surface structure (nature and density of the surface sites).¹⁸ Thus, the voltammetric features at 0.12, 0.27, 0.37, and 0.53 V vs RHE are characteristic of the presence of (110) sites, (100) steps and terrace borders, (100) terraces or wide domains, and (111) sites, respectively. The main trend observed in Figure 1 is the increase of (100) sites, especially the (100) terraces, when the amount of HCl increases up to 25%. The increase of this type of surface site is counterbalanced by a decrease of the (110) and (111) sites. Interestingly, the amount of (111) sites is nearly negligible for the nanoparticles prepared with 25% HCl. For higher HCl concentrations, the amount of (100) terraces again decreases while the other orientations concurrently increase.

Previous contributions pointed out that a voltammetric profile similar to that obtained with 25% HCl is characteristic of cubic Pt nanoparticles.^{13,18} To verify this point, TEM measurements were carried out. Figure 2 shows a representative TEM image of the Pt

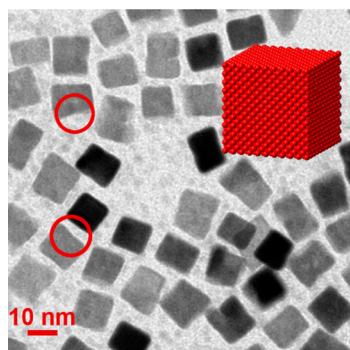


Figure 2. TEM image of platinum nanoparticles prepared by water-in-oil microemulsion in the presence of 25% HCl in the aqueous phase. Red open circles show the etching effect of HCl.

nanoparticles obtained with 25% HCl. The presence of Pt cubes with a particle size of about 12–14 nm is confirmed. These cubes are ideally enclosed by six {100} faces,¹⁹ which appear clearly reflected in the voltammetric profile in the potential range between 0.3 and 0.45 V (Figure 1, dark blue line). The evolution of the shape of the nanoparticles in the entire range of HCl percent is shown in Figure S1 (Supporting Information).

Between 0 and 25% HCl, a clear evolution from quasi-spherical to cubic particles is observed. Liz-Marzán and co-workers recently made a similar observation on Au@Ag nanoparticles. They observed, in the presence of halide ions, a preferential formation of Ag {100} facets on gold, regardless of the starting gold morphology, as predicted by density functional theory (DFT) surface energy calculations.²⁰ In addition, the particle size increased from 3 to 5 nm (0% HCl) to 12–14 nm (25% HCl). However, from this percentage of HCl to the maximum value studied (37% HCl), TEM images show an evolution from cubes to bonelike Pt nanoparticles. This evolution could be ascribed to the HCl etching properties.²¹ In fact, some etching can already be observed for some cubes and is marked with red open circles in Figure 2. In terms of particle size, it remains nearly constant (about 12–14 nm) for these higher HCl percentages.

In order to quantitatively measure the amount of (100) sites at the surface of the different Pt nanoparticles, two different methods have been employed: hydrogen adsorption/desorption deconvolution¹⁸ and germanium irreversible adsorption.^{18,22} However, it is important to note the differences between these two approaches. Thus, while for the former all sites with (100) geometry, that is both step and terraces can be quantified, in the latter only those having wide enough surface domains for Ge to be adsorbed (each atom needs four platinum atoms) will be detected. Consequently, this second method will always give lower values, because both (100) steps and terraces with less than four Pt atoms will be undetectable. Figure 3 shows the percentage of (100) surface sites obtained for the Pt nanoparticles prepared with different amounts of HCl.

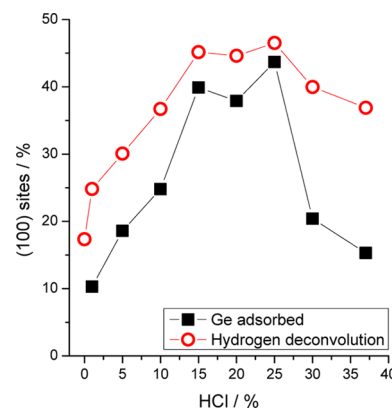


Figure 3. Amount of (100) sites measured by Ge irreversible adsorption (solid black squares) and by hydrogen adsorption/desorption deconvolution (open red circles) for different HCl% in the aqueous phase of water-in-oil microemulsion.

As expected, the amount of (100) surface sites provided by the deconvolution analysis is always higher than that obtained with the Ge analysis. However, both analyses show a similar trend: that is, an increase of the (100) sites from 0 to 25% HCl and then a clear decrease from 25 to 37% HCl. In addition, it is important to point out the good agreement between these two analyses for the samples containing a higher fraction of (100) terraces (from 15 to 25% HCl), whereas for those samples containing a higher fraction of (100) step sites (from 0 to 15% HCl and from 25 to 37% HCl), important differences are found, as expected from the particular requirements of the analysis. In fact, from both analyses, it is possible to estimate the (100) terrace to total (100) site ratio for each Pt sample. Thus, for instance, whereas in the range of 15–37% HCl the total numbers of (100) surface sites

are rather similar (47–37%), the percentages of (100) terraces are very different, ranging from 44% (25% HCl) to 15% (37% HCl). Therefore, nearly all (100) sites for the 25% HCl nanoparticles are present as wide (100) domains, while for the 37% HCl nanoparticles (100) steps and defects are more abundant than (100) wide terraces. Finally, in terms of the highest amount of (100) surface sites, the value of (100) sites for the 25% HCl is similar (44%) to those previously reported for cubic nanoparticles synthesized with the colloidal method.^{3,23}

To understand which factors are responsible for the formation of the cubic Pt nanostructures in the presence of HCl, additional experiments were performed in which the independent effect of the presence of Cl^- ions or protons was evaluated. Thus, for the former, the synthesis was carried out with the addition of NaCl in the aqueous phase with a Cl^- concentration equal to that of 15% HCl. On the other hand, to study the effect of protons, another synthesis was undertaken but with 15% HClO_4 in the aqueous phase (perchlorate anions are known to be weakly adsorbed on Pt surfaces). From the voltammetric response of these samples (see Figure S4, Supporting Information), it is evident that none of these experiments induced the formation of a preferential (100) surface structure. Thus, a combined effect of Cl^- ions and low pH values seems to be the responsible for the formation of the Pt cubes. In relation to the individual effects of protons and chloride in the reduction time, it was observed that increasing amounts of the latter made the reaction more sluggish but always within 10 min, while changes in the pH did not have any significant effect in the reduction time. More work is in progress to understand the particular effect of these species on the growth rate of the nanoparticles.

To evaluate the electrocatalytic properties of the Pt nanoparticles, ammonia electro-oxidation in alkaline solution has been studied. This is an interesting reaction not only due to its possible application as ammonia-based low-temperature fuel cells but also as source of production of high-purity hydrogen, among others. Very interestingly, this anodic reaction has been shown to be extremely sensitive to the surface structure on platinum, taking place almost exclusively on (100) sites and being also sensitive to the width of the (100) terraces.^{15,16} In fact, cubic Pt nanoparticles prepared using colloidal routes have already illustrated how the electrocatalytic activity can be optimized by controlling the surface structure of the catalytic material. Consequently, this reaction is an excellent candidate to test the electrocatalytic properties of the different samples. Figure 4A shows the voltammetric response of the collection of Pt samples toward ammonia oxidation. The results obtained clearly show that the activity for the different nanoparticles follow the same trend than that observed for the amount of (100) surface sites at the nanoparticles measured by germanium irreversible adsorption. Remarkably, a 6-fold increase in the ammonia oxidation current density is observed from 0% to 25% HCl. However, it is worth noting that this reaction is also very sensitive to the width of the (100) terraces. Thus, for instance, and despite the fact that the total amount of (100) sites of the sample prepared in the presence of 5% HCl is lower than that obtained with the samples prepared in the range between 30 and 37% of HCl, their activities toward ammonia oxidation are rather similar. This finding is in agreement with the analysis of the amount of (100) terraces of these samples (Figure 3), which is similar in both cases.

Moreover, in terms of the maximum current densities, the Pt nanoparticles prepared with 25% HCl (about 1.96 mA cm^{-2}) show values higher than those reported for Pt nanoparticles

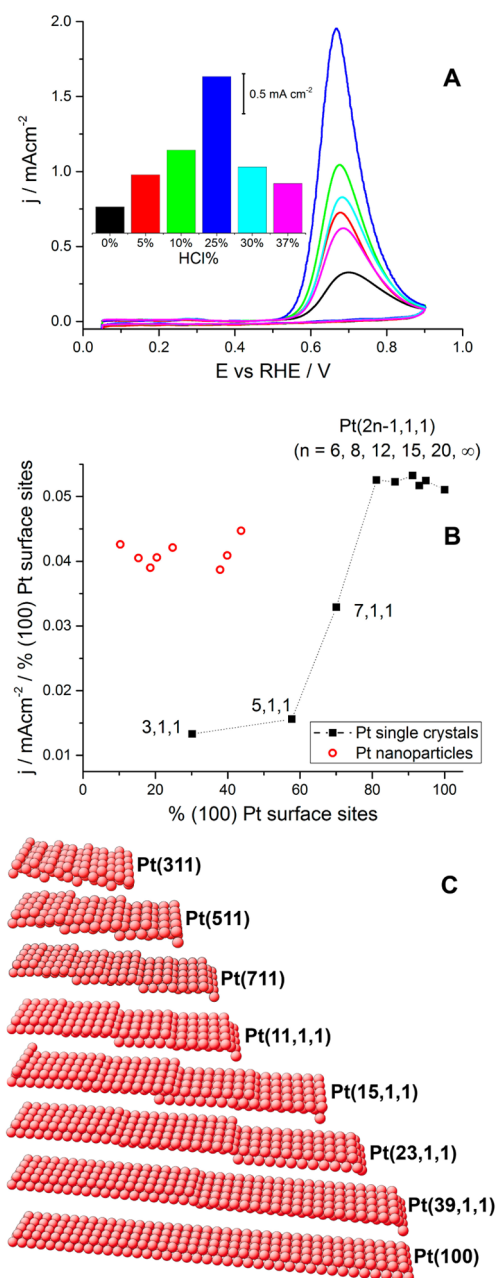


Figure 4. (A) Voltammetric profiles for ammonia oxidation with platinum nanoparticles prepared by water-in-oil microemulsion in the presence of different amounts of HCl. The inset shows the current density of the main peak versus the amount of HCl. (B) Normalized current density for $\text{Pt}(2n-1,1,1)$ single crystals ((100) terraces with (111) steps) and platinum nanoparticles prepared with different amounts of HCl in the aqueous phase of the microemulsion: test solution, 0.2 M NaOH + 0.1 M NH_3 ; scan rate, 10 mV s^{-1} . (C) Atomic representation of stepped Pt surfaces with (100) terraces and (111) steps.

prepared with a colloidal method using sodium polyacrylate.^{12–14} Consequently, this current density is at present the highest reported so far in the literature for ammonia oxidation at room temperature.

Finally, with the objective of analyzing in more detail the effect of the size of (100) domains present at the surface of the Pt nanoparticles, we have normalized their catalytic activity to the amount of wide (100) sites determined by Ge irreversible adsorption, shown in Figure 3 (black squares). A similar

rationalization was also done with Pt single crystals with stepped surfaces (Pt(2n-1,1,1) single crystals ((100) terraces with (111) steps)) (Figure S4, Supporting Information). Both calculations are plotted and compared in Figure 4B. For the stepped Pt surfaces, the tremendous influence of the (100) terrace width is clear. Larger (100) terraces are proportionally much more active than shorter terraces, denoting a clear sensitivity to the long-range order of (100) surface domains. Nevertheless, it is also important to stress that this long-range order effect is particularly sensitive to the transition between three (Pt(511)) and six (Pt(11,1,1)) terrace atoms. However, for surfaces with terrace widths of six or more atoms the normalized current densities are independent of the terrace width. In the case of the Pt nanoparticles (Figure 4B, red open circles), we observe that the activity normalized to the (100) wide sites is nearly the same and is similar to those single crystals having terrace widths of $4 < n < 6$ atoms. This fact could be related to the presence of (100) domains with these dimensions on the nanoparticles. However, one should take into account that, due to the lower percentage of (100) terraces on the nanoparticles, their maximum activity (~ 2 mA cm⁻²) is lower than that expected from stepped single crystals of similar (100) terrace width (Figure S5, Supporting Information).

In conclusion, this work shows a fast, easy, room-temperature, and scalable procedure of synthesis of cubic Pt nanoparticles based on the reduction of a Pt precursor by NaBH₄ in a water-in-oil microemulsion in the presence of HCl. The percentage of HCl is the key point in controlling the shape/surface structure of the Pt nanoparticles. TEM and cyclic voltammetry measurements confirm the presence of Pt cubes with a preferential (100) surface structure. Different electrochemical probes have been used to quantify the total amount of (100) surface sites as well as to quantify the amount of (100) terraces present at the nanoparticles. The optimal amount of HCl was found to be between 15 and 25%, after which the samples show a decrease in the number of (100) wide domains as well as a bonelike shape. The electrocatalytic activity of the samples was tested toward ammonia oxidation. The activity reported with 25% HCl was about 6 times higher than that obtained with 0% HCl. This activity is currently the largest quantified current density so far in the literature. More work is currently in progress to extend this methodology to prepare other shape-controlled metal nanoparticles such as Pd and Rh as well as to obtain shape-controlled Pt alloys. In particular, the use of shape-controlled Pt alloys for the oxygen reduction reaction has been the subject of intense research in the last few years.²⁴⁻²⁶

■ ASSOCIATED CONTENT

📄 Supporting Information

Text and figures giving experimental details describing NP syntheses, TEM analyses, area normalization, effect of Cl⁻ and pH on the shape of the Pt nanoparticles, and ammonia oxidation on several Pt single crystals. This material is available free of charge via the Internet at <http://pubs.acs.org>.

■ AUTHOR INFORMATION

Corresponding Author

jose.solla@ua.es

Notes

The authors declare no competing financial interest.

■ ACKNOWLEDGMENTS

This work has been financially supported by the MCINN-FEDER (Spain) (project CTQ 2010-16271), by the Generalitat Valenciana (project PROMETEO/2009/045), and in part by the NASA-URC Grant No. NNX10AQ17A and NSF-NSEC Center for Hierarchical Manufacturing Grant No. CHM-CMMI-0531171. R.M.-R. is grateful to the Becas Iberoamérica, Santander Universidades-España 2012, and PR-LSAMP Bridge to Doctorate Fellowship programs.

■ REFERENCES

- (1) Long, N. V.; Chien, N. D.; Hayakawa, T.; Hirata, H.; Lakshminarayana, G.; Nogami, M. *Nanotechnology* **2010**, *21*.
- (2) Tao, A. R.; Habas, S.; Yang, P. *Small* **2008**, *4*, 310.
- (3) Vidal-Iglesias, F. J.; Aran-Ais, R. M.; Solla-Gullon, J.; Herrero, E.; Feliu, J. M. *ACS Catal.* **2012**, *2*, 901.
- (4) Zhou, Z. Y.; Shang, S. J.; Tian, N.; Wu, B. H.; Zheng, N. F.; Xu, B. B.; Chen, C.; Wang, H. H.; Xiang, D. M.; Sun, S. G. *Electrochem. Commun.* **2012**, *22*, 61.
- (5) Narayanan, R.; El-Sayed, M. A. *Nano Lett.* **2004**, *4*, 1343.
- (6) Narayanan, R.; El-Sayed, M. A. *J. Phys. Chem. B* **2004**, *108*, 5726.
- (7) Ahmadi, T. S.; Wang, Z. L.; Green, T. C.; Henglein, A.; El-Sayed, M. A. *Science* **1996**, *272*, 1924.
- (8) Tian, N.; Zhou, Z.-Y.; Sun, S.-G.; Ding, Y.; Wang, Z. L. *Science* **2007**, *316*, 732.
- (9) Xiao, J.; Liu, S.; Tian, N.; Zhou, Z.-Y.; Liu, H.-X.; Xu, B.-B.; Sun, S.-G. *J. Am. Chem. Soc.* **2013**, *135*, 18754.
- (10) Mihaly, M.; Fleancu, M. C.; Olteanu, N. L.; Bojin, D.; Meghea, A.; Enachescu, M. C. R. *Chim.* **2012**, *15*, 1012.
- (11) Hernández, J.; Solla-Gullón, J.; Herrero, E. *J. Electroanal. Chem.* **2004**, *574*, 185.
- (12) Vidal-Iglesias, F. J.; Solla-Gullón, J.; Montiel, V.; Feliu, J. M.; Aldaz, A. *J. Power Sources* **2007**, *171*, 448.
- (13) Vidal-Iglesias, F. J.; Solla-Gullón, J.; Rodríguez, P.; Herrero, E.; Montiel, V.; Feliu, J. M.; Aldaz, A. *Electrochem. Commun.* **2004**, *6*, 1080.
- (14) Solla-Gullón, J.; Vidal-Iglesias, F. J.; Rodríguez, P.; Herrero, E.; Feliu, J. M.; Clavilier, J.; Aldaz, A. *J. Phys. Chem. B* **2004**, *108*, 13573.
- (15) Vidal-Iglesias, F. J.; Garcia-Araez, N.; Montiel, V.; Feliu, J. M.; Aldaz, A. *Electrochem. Commun.* **2003**, *5*, 22.
- (16) Vidal-Iglesias, F. J.; Solla-Gullón, J.; Montiel, V.; Feliu, J. M.; Aldaz, A. *J. Phys. Chem. B* **2005**, *109*, 12914.
- (17) Solla-Gullón, J.; Vidal-Iglesias, F. J.; López-Cudero, A.; Garnier, E.; Feliu, J. M.; Aldaz, A. *Phys. Chem. Chem. Phys.* **2008**, *10*, 3689.
- (18) Solla-Gullón, J.; Rodríguez, P.; Herrero, E.; Aldaz, A.; Feliu, J. M. *Phys. Chem. Chem. Phys.* **2008**, *10*, 1359.
- (19) Zhou, Z.-Y.; Tian, N.; Huang, Z.-Z.; Chen, D.-J.; Sun, S.-G. *Faraday Discuss.* **2009**, *140*, 81.
- (20) Gómez-Graña, S.; Goris, B.; Altantzis, T.; Fernández-López, C.; Carbó-Argibay, E.; Guerrero-Martínez, A.; Almora-Barrios, N.; López, N.; Pastoriza-Santos, I.; Pérez-Juste, J.; Bals, S.; Van Tendeloo, G.; Liz-Marzán, L. M. *J. Phys. Chem. Lett.* **2013**, *4*, 2209.
- (21) Liu, M.; Zheng, Y.; Zhang, L.; Guo, L.; Xia, Y. *J. Am. Chem. Soc.* **2013**, *135*, 11752.
- (22) Rodríguez, P.; Herrero, E.; Solla-Gullón, J.; Vidal-Iglesias, F. J.; Aldaz, A.; Feliu, J. M. *Electrochim. Acta* **2005**, *50*, 4308.
- (23) Vidal-Iglesias, F. J.; Solla-Gullon, J.; Herrero, E.; Aldaz, A.; Feliu, J. M. *Angew. Chem., Int. Ed.* **2010**, *49*, 6998.
- (24) Zhang, J.; Yang, H.; Fang, J.; Zou, S. *Nano Lett.* **2010**, *10*, 638.
- (25) Cui, C.; Gan, L.; Li, H. H.; Yu, S. H.; Heggen, M.; Strasser, P. *Nano Lett.* **2012**, *12*, 5885.
- (26) Choi, S. I.; Xie, S.; Shao, M.; Odell, J. H.; Lu, N.; Peng, H. C.; Protsailo, L.; Guerrero, S.; Park, J.; Xia, X.; Wang, J.; Kim, M. J.; Xia, Y. *Nano Lett.* **2013**, *13*, 3420.